AGU PUBLICATIONS

Geophysical Research Letters

RESEARCH LETTER
10.1002/2014GL061604

Key Points:
- Infragravity wave are tracked across oceans using DART data and a model
- Sources of the largest infragravity wave events are analyzed
- The largest IG waves in the west Pacificoriginate from the east Pacific

Supporting Information:
- Readme
- Figure S1

Correspondence to:
A. Rawat,
arawat@ifremer.fr

Citation:
Rawat, A., F. Ardhuin, V. Ballu, W. Crawford, C. Corela, and J. Aucan (2014), Infragravity waves across the oceans, *Geophys. Res. Lett.*, *41*, 7957–7963, doi:10.1002/2014GL061604.

Received 3 OCT 2014
Accepted 23 OCT 2014
Accepted article online 28 OCT 2014
Published online 25 NOV 2014

Infragravity waves across the oceans

Arshad Rawat[1,2], Fabrice Ardhuin[1,3], Valérie Ballu[4], Wayne Crawford[4,5], Carlos Corela[6], and Jerome Aucan[7]

[1]Ifremer, Laboratoire d'Océanographie Spatiale, Brest, France, [2]Mauritius Oceanography Institute, Mauritius, [3]Laboratoire de Physique de Oceans, UMR 6523, CNRS-IFREMER-IRD-UBO, Plouzané, France, [4]LIENSs, UMR 7266, CNRS/Université de la Rochelle, France, [5]IPGP, Pres Univ. Paris Sorbonne Cité, France, [6]Instituto Dom Luiz, Lisbon, Portugal, [7]Institut de Recherche pour le Développement (IRD), Nouméa, New Caledonia

Abstract Ocean infragravity (IG) waves are low-frequency waves generated along shorelines by incident seas and swell and with heights of the order of 1 cm in the open ocean. Despite these small amplitudes, they can be of much importance for ice shelf break up and errors in measurements of sea level by future satellite altimeters. A combination of numerical model results and in situ data is used to show that bottom pressure signals in the infragravity frequency band can be dominated by bursts of energy that travel across ocean basins, and can last for several days. Two particularly strong events recorded in 2008 are studied, one in the North-Pacific and the other in the North-Atlantic. It is shown that infragravity waves can travel across whole oceans basins with the signal recorded on the western shores often dominated by IG waves coming from the opposite shore of that same ocean basin.

1. Introduction

Infragravity (IG) waves are long surface gravity waves with typical periods of 30 s to 5 min. The IG wave field contains both free waves, with dispersion properties given by linear wave theory, and bound waves resulting from the local sub-harmonic interaction of wind seas and swells [*Biesel*, 1952]. Measurements with arrays of instruments reveal that free waves generally dominate the bottom pressure records in water depths larger than 20 m or so [*Webb et al*., 1991; *Herbers and Guza*, 1991, 1992]. Integrated over 5 to 30 mHz, the heights of IG waves strongly vary with the local water depth, ranging from an average of 0.5 to 2 cm in 4000 m depth [*Aucan and Ardhuin*, 2013] to several meters during extreme events near the shoreline where they play an important role in coastal flooding [*Sheremet et al*., 2014]. The possible resonant excitation of harbors [e.g., *Okihiro et al*., 1993] and ice tongues [*Bromirski et al*., 2010] means that even small amplitudes IG waves can be important. The renewed interest in IG waves studies comes from future satellite altimeter missions with improved resolution and accuracy that are planning to measure sea level variations within meso- and submeso-scale features (such as fronts and filaments) and their associated ocean currents [e.g., *Alsdorf et al*., 2007]. At wavelengths around 10 km, these features may often be obscured by IG waves when observed by a satellite altimeter [*Ardhuin et al*., 2014]. These recent developments call for a quantitative understanding of IG wave properties at global geographical scales, and at event-like temporal scales.

The detailed analysis of IG waves started with *Munk* [1949] and *Tucker* [1950]. It is now known that nonlinear interactions among wind waves or swell generally explain the generation of IG waves. These interactions can be the amplification of second-order sub-harmonics in shallow water [cf. *Holman and Bowen*, 1984; *Holtman-Shay and Guza*, 1987], and/or the low-frequency wave generation by the variation of the position where short waves break [*Symonds et al*., 1982]. The dissipation of IG waves is not well known and probably combines bottom friction and the exchange of energy between short and long waves [*Thomson et al*., 2006]. In our model the dissipation is only significant on the continental shelves, consistent with sensitivity analyses of tsunami propagation [*Dao and Tkalich*, 2007], which are similar surface gravity waves. More specifically, our model results with bottom friction de-activated for depths larger than 500 m are not distinguishable from model results with bottom friction acting everywhere.

Extensive observations, in particular on the Pacific and Atlantic continental shelves, show a strong correlation between infragravity and swell energy levels, suggesting that free infragravity waves are generally radiated from nearby beaches [*Herbers et al*., 1995]. Observed infragravity energy levels on the beach, shelf, and in the open ocean are consistent with a strong refractive trapping of free wave energy, which decay inversely with

©2014. American Geophysical Union. All Rights Reserved.

depth in shallow water [e.g., *Webb et al*., 1991; *Okihiro et al*., 1993; *Herbers et al*., 1995]. A small fraction of IG energy can escape to the open ocean and arrive at remote shorelines. Indeed, deep ocean measurements using arrays of pressure recorders show the propagation of free IG waves coming from shorelines exposed to storms [*Webb et al*., 1991; *Harmon et al*., 2012; *Godin et al*., 2014]. These "leaky waves" are likely responsible for a persistence of IG wave energy even when local short waves are weak.

The objective of the present paper is to investigate the generation and the propagation from coast to coast of high energy free IG wave events. The seasonal average IGW fields have already been investigated by using in situ data *Aucan and Ardhuin* [2013] and numerical simulations [*Ardhuin et al*., 2014]. Here, our focus on the strongest IGW events is motivated by several applications in which these events are important: this is the case for the question of precise satellite altimetry measurements or the breaking of ice tongues off Antarctica [*Bromirski et al*., 2010]. For example for the upcoming Surface Water and Ocean Topography (SWOT) mission, the determination of the strongest "noise" in sea level measurement coming from IG waves will be crucial, especially during these major IG bursts.

A detailed comparison between predictions and observations is made over ~10 day periods corresponding to a major storm in the Pacific and another major storm in the Atlantic. The model and data analysis method is briefly reviewed in section 2, followed by a detailed analysis of the two IG events in section 3, a thorough discussion in section 4, and a conclusion in section 5.

2. Methods: Numerical Model and Data Processing

2.1. Model

Our numerical model for infragravity waves represents the spectral evolution of the free IG waves by a simple extension to low frequencies of the usual spectral wave models used for wind seas and swell. A source of IG wave energy is parameterized from the shorter wave components at all grid points adjacent to land. All these aspects are described in details by *Ardhuin et al*. [2014] and are included in the version 4.18 of the WAVEWATCH III modeling framework [*Tolman et al*., 2014]. The important aspect of this model is the source of IG free waves, which was inferred empirically from coastal measurements in Hawaii, North Carolina, and France. Based on these data sets, the IG wave height H_{IG} radiated from the shoreline was set to

$$H_{IG} \approx \alpha_1 H_s T_{m0,-2}^2 \sqrt{\frac{g}{D}} \tag{1}$$

where H_s is the significant wave height of wind seas and swells, $T_{m0,-2}$ is the mean period given by the -2 and 0 moments of the surface elevation spectrum, g is the apparent acceleration of gravity, D is the local mean water depth, and α_1 is a dimensional constant. The choice of wave period $T_{m0,-2} = (m_0/m_2)^{1/2}$ with the nth moment $m_n = \int_0^{\infty}\int_0^{2\pi} f^n E(f,\theta) df d\theta$, is relatively arbitrary (f being the frequency and $E(f,\theta)$ the directional wave spectrum). Basically, it is less noisy than the usual peak period and gives more importance to the low frequency part of the spectrum than other mean periods defined from the -1 or +1 moments. The observation analyzed by *Ardhuin et al*. [2014] shows that, within a factor of 2, $\alpha_1 = 12 \times 10^{-4}\ s^{-1}$. This constant value was used in our present model. Equation (1) was extended to any water depth by replacing D by the proper amplification factor for a broad directional wave spectrum for which the energy is conserved.

We further assume that an equal amount of energy is radiated in all directions. This and an empirical distribution across frequencies f provide a value of the directional wave spectrum $E_{IG}(f,\theta)$ that is prescribed in the model at all points adjacent to land The wavenumber k and frequency f are related by the dispersion relation $(2\pi f)^2 = gk \tanh(kD)$.

The validation of this model was shown for a few locations in *Ardhuin et al*. [2014]. The same settings are used here, with a spatial resolution of 0.5 degree in latitude and longitude, a model spectral band that ranges from 0.003 to 0.72 Hz, and a forcing that includes ECMWF operational wind analyses, NCEP sea ice concentrations, and small icebergs concentrations for the southern ocean from Ifremer/CERSAT which reduce the wave energy flux [*Ardhuin et al*., 2011].

2.2. Observations

We use bottom pressure records from a few more stations, including permanent Deep-ocean Assessment and Reporting of Tsunamis (DART) stations, the pressure time series from the MOMAR

©2014. American Geophysical Union. All Rights Reserved.

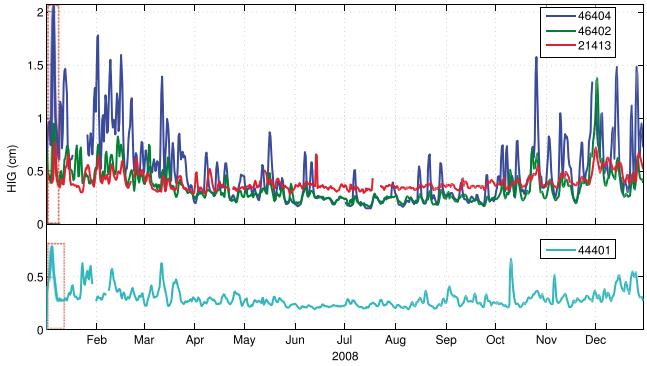

Figure 1. Time series of infragravity (IG) levels measured at (a) Deep-ocean Assessment and Reporting of Tsunamis (DART) stations 46404 (off Oregon), 46402 (off Alaska), and 21413 (off Japan), all in the North Pacific and (b) DART station 44401 in the Atlantic. The red boxes mark the two events that are studied in detail. Pressure values were translated into surface elevation for the frequency range 5 to 10 mHz and the temporal resolution is 6 h.

(Monitoring of the Mid-Atlantic Ridge) Observatory [*Ballu et al*., 2009], and the NEAREST campaign off the continental margin of Portugal [*Harris et al*., 2013], including broadband hydrophones HTI-01-PCA/ULF digitized and logged in Geolon MCS recorders. Ocean bottom pressure records are transformed into infragravity wave elevation parameters by computing Fourier transform over 30 min overlapping windows averaged every 3 h.

After correcting for the instrument response, the bottom power pressure spectrum $F_p(f)$ was converted to a surface elevation spectrum $E(f)$, assuming that all the recorded signal corresponds to (free) linear surface gravity waves as in *Aucan and Ardhuin* [2013],

$$E(f) = F_p(f)\left(\frac{cosh(kD)}{\rho g}\right)^2 \tag{2}$$

This transformation is appropriate if the linear wave signal dominates, and if it is above the instrument noise floor. These constraints limit the validity of equation (2) to a finite range of frequencies between f_{min} and f_{max}. To avoid other types of motions we chose $f_{min} = 5$ mHz, and to be able to compare data from all water depths, up to 5800 m, we set $f_{max} = 10$ mHz. Over these frequencies we define an infragravity wave height, by analogy with the usual significant wave height,

$$H_{IG} = 4\sqrt{\int_{f_{min}}^{f_{max}} E(f) - E_N df} \tag{3}$$

where E_N is a noise floor that was adjusted to the median of the spectral density at 15 mHz for each measurement location. We also estimated this height from the modeled spectra $E(f)$ using the same expression. In that case there is no noise and we use $E_N = 0$. All previous studies have shown that at depths greater than a few hundred meters, the bound infragravity waves are negligible compared to the free waves [e.g., *Webb et al*., 1991; *Herbers et al*., 1994]. We can thus compare directly the model results for $E(f)$ or H_{IG} to the measurements.

Because most high resolution data are not available from DART stations after the year 2008, and because the numerical wave model is most reliable for recent years when winds are best known [e.g., *Rascle and Ardhuin*, 2013], we have thus focused on the year 2008 and chosen the most energetic events for each of the North Pacific and the North Atlantic regions.

Observations shown in Figure 1 are for DART station 46404, 46402, and 21413 in the Pacific Ocean and DART station 44401 in the Atlantic Ocean cover both winter and summer seasons. Many peaks in all three Pacific time series appear to coincide, especially during winter months, revealing that IG bursts are not localized events but can be coherent at the scale of ocean basins. A comprehensive analysis of the year 2008 (Supporting information figure) shows a good correlation between the peak levels recorded at DART stations 46407 and 21413 within a time lag of about 20 h. The next section will focus on the most energetic events of

©2014. American Geophysical Union. All Rights Reserved.

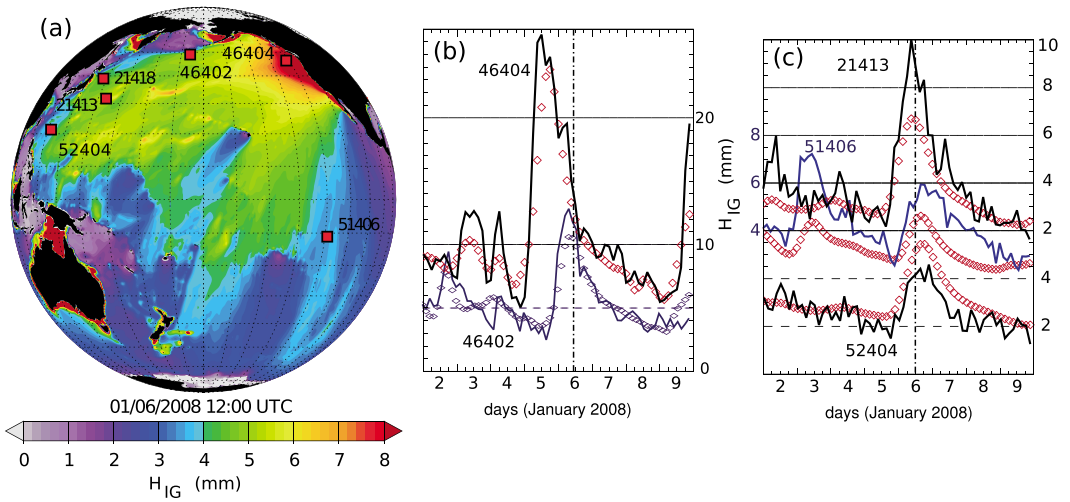

Figure 2. (a) Modeled infragravity wave heights at 12:00 UTC on 06/01/2008 over the Pacific Ocean with locations of pressure sensors used (red squares). (b) HIG measured (solid lines) and modeled (symbols) at DART stations close to the North American shorelines. (c) HIG measured (solid lines) and modeled (symbols) at remote DART stations, the curves have been offset vertically. Pressure measurements were translated into surface elevation using equations (4)–(5). The vertical dash-dotted line in Figures 2b and 2c marks the time of the map shown in Figure 2a.

the year 2008, one in the north Pacific, and one in the north Atlantic, that are representative of all the events for which the IG wave height reaches over 0.8 cm, when computed over the range 5 to 10 mHz.

3. IG Waves Across the Pacific

A major storm developed rapidly in the North Pacific and hit the Eastern Pacific coasts from Canada to Mexico on 5 January 2008, with offshore wave heights in excess of 10 m, and peak periods of around 17 s. These large periods, high wave heights, and the storm's large spatial extent combine to produce the largest source of infragravity signal recorded in 2008 at DART station 46404, located 4000 km offshore of Oregon at 2800 m depth. As defined by equation (3), the IG wave height at the surface is estimated at 27 mm over the frequency band 5 to 10 mHz. Station 46407, located 400 km to the south, also reported the highest value for that year during that event, with 31 mm. Across the Pacific, there is a clear IGW event occurring on 6 January (Figure 2), with heights of 5 mm at Pitcairn Island, in the Central Pacific (DART station 51406), 5 mm near the Philippines (station 52404), and 7 to 9 mm off Japan (stations 21413 and 21418). For these three west Pacific stations, these are the highest values recorded over the period January to March 2008. The same is true for the Aleutian island station 46408 with 13 mm recorded near 0 UTC on 6 February. In contrast, the Hawaii station 51407, located 60 km west of Big Island, did not record anything particular on 6 January, probably due to the masking effect of the island. Based on these measurements alone, it is very difficult to associate these records with a single event. It is the numerical model, as shown on Figure 2a, that brings a clear picture of a coherent IG wave field forming on 5 January in the north-east Pacific and radiating across the oceans over the next 2 days. The model gives a picture of the IG wave heights that is strongly blocked by islands chains and amplified by mid-ocean topographic features. That amplification is due to the shoaling of these long waves when the water depth decreases. Infragravity waves have periods that are only a few times shorter than those of large tsunamis. IG and tsunami waves thus have very similar propagation speeds and spatial distributions of amplitudes caused by shoaling and refraction.

These model gradients are difficult to validate with the few data available. Still, the general pattern of lower wave heights to the south of the source and higher wave heights to the west is very well captured by the model, together with the timing of the IG wave arrival.

Contrary to many coastal shallow water sites that are often dominated by local IG waves, the deep ocean records in the west Pacific are thus dominated by IG waves that have traveled across the ocean basin. These remote IG waves are easily detected due to the lower levels of regionally generated IG energy. This lower

©2014. American Geophysical Union. All Rights Reserved.

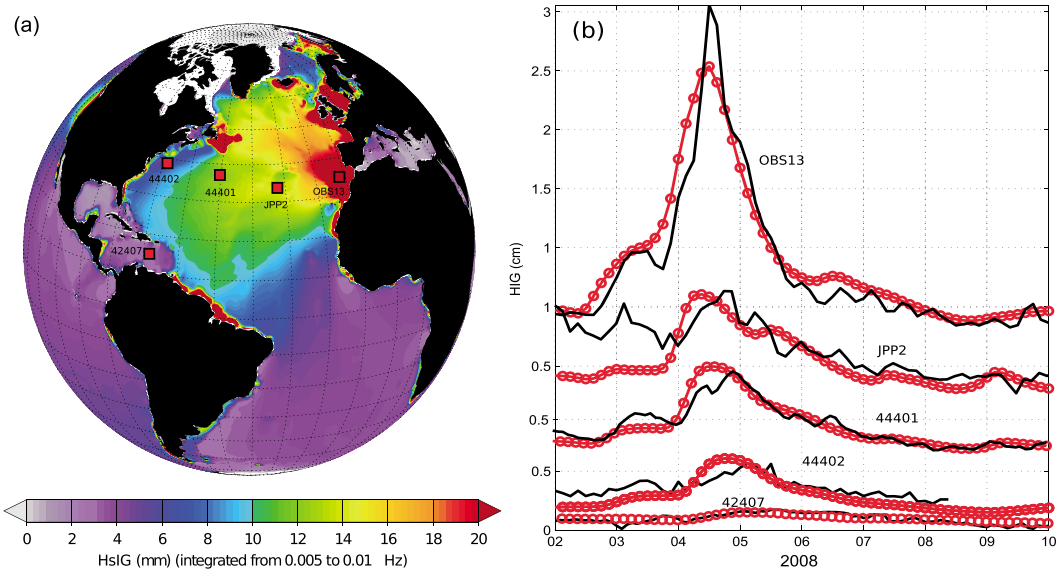

Figure 3. (a) Modeled instantaneous IG wave field on 6 January 2008 over the North-Atlantic Ocean with locations of pressure sensors used (red squares). (b) IG levels measured (black lines) and modeled values (red lines and circles) for the corresponding station. Pressure values were translated into surface elevation for the frequency range 5 to 10 mHz.

level, following equation (1), is the result of lower incident wave heights and shorter wave periods along the western boundaries of the Pacific basin.

4. IG Waves Across the North Atlantic

A massive North-Atlantic winter storm developed off Newfoundland on 2 January 2008, and generated waves with heights exceeding 15 m in the middle of the north Atlantic by the evening of 2 January. High waves arrived in Portugal and Morocco, between 3 and 4 January, with wave heights exceeding 10 m and peak periods around 20 s. The model predicts an IG burst propagating across the basin from the Eastern coasts to the Western coasts of the Atlantic (Figure 3a).

The model predicts IG waves with heights larger than 1 cm in deep water from Brazil to Iceland. These predictions are generally consistent with the few data available. There is even a clear maximum that exceeds 2 mm in the Caribbean Sea south of Puerto Rico (DART station 42407), which occurs at the time predicted by the model.

Only three DART stations had available records in the North Atlantic. These were supplemented by two additional observations collected as part of the geophysical experiment NEAREST and the seafloor pressure time series collected in the framework of the MoMAR Observatory [*Ballu et al*., 2009]. In the context of the NEAREST project, broadband ocean bottom seismometers and hydrophones (OBS) were deployed in the Gulf of Cadiz for the period of September 2007 to August 2008. The OBS13 sensor was deployed at the Gulf of Cadiz, at a depth of around 4500 m. It is situated close to the source of the IG event and recorded a maximum height of 3.0 cm which coincides with the maximum modeled value of 2.5 cm. Model estimates of H_{IG} at DART stations 44401 and 42407 are also in good agreement with the measurements. Discrepancies are more important at station 44402, off the U.S. coast.

The spatial distribution of IG wave heights is marked by a strong shoaling and refraction across the Grand Banks, off Newfoundland. As a result, the U.S. East coast, including station 44402, receives a much lower level of IG energy. The shadowing effect of the Azores can also be noticed. The model also predicts an important amplification over the mid-Atlantic ridge, with values that are consistent with measurements made at the MoMAR Observatory JPP2 site. Before the IG event, the model underestimates the energy levels on 2 and 3 January at JPP2 and 44401. These are, according to the model, caused by the previous storm which hit the Portuguese coast on 2 January. This model underestimation at JPP2 may be the result of an exaggerated sheltering by the Azores. According to the model, the 4 January event is the largest source of IG waves for

©2014. American Geophysical Union. All Rights Reserved.

that month, for most locations in the North Atlantic with depth larger than 2000 m, in the latitude band 5°N to 55°N, including the Caribbean sea, but excluding the Gulf of Mexico which was rather sheltered from this event.

5. Discussion

Both of the infragravity wave events highlighted here are caused by long period swells from extratropical storms with predominant westerly winds and waves. Waves propagating from east to west can also generate IG waves on western boundaries. However, given the scaling of the IG source with wave height and mean period squared, the sources off western boundaries of the Pacific and Atlantic Oceans are much weaker in general. Compared to the extratropical depressions, even hurricane waves are generally too small and with too short periods to generate comparable IGW bursts. From the model runs used and available observations, few sources of strong IG event were found in the equatorial regions. For example, in 2008 only one clear event was observed at DARTs 42407, 44401, and 41424 around 19 March 2008. This event was noticeable in the region around Puerto Rico and the U.S. Virgin Islands. It was not associated with a tropical storm but rather to unusual long swell generation by an extratropical storm. This is the "Extreme Atlantic Swell Event of March 2008" analyzed by *Lefevre* [2009] and *Cooper et al*. [2013]. Another similar case of "high swell from a remote storm" caused widespread flooding in western Pacific islands [*Hoeke et al*., 2013] on 10 December 2008.

IG generation in general is not limited to these storms and hurricanes, and any interaction of short waves with the coastlines will produce IG waves, but their energy can be several orders of magnitude less than in the cases selected here. It is the intensity, duration, and trajectory of the winter storms that define the largest wave heights and periods [e.g., *Hanafin et al*., 2012] and give rise to the strongest IG bursts.

6. Conclusion

We have shown that free infragravity (FIG) waves radiating from coastlines along the eastern boundaries of ocean basins are the origin of the largest energy bursts in the infragravity band (here restricted to 5–10 mHz). Free IG waves are recorded by the global network of bottom pressure recorders used for tsunami warning, and other geophysical experiments using pressure gauges or hydrophones. The large FIG events are also well predicted by our spectral numerical model which uses empirical free infragravity sources determined from wind sea and swell properties all along the world's shorelines [*Ardhuin et al*., 2014].

Previous studies were based on the analysis of a single array at one location and estimated likely position and sometimes strengths of sources of the IG waves [*Webb et al*., 1991; *Harmon et al*., 2012]. Here we have combined scattered in situ observations and a global numerical model to demonstrate the trans-oceanic propagation of IG waves, which has not been explicitly documented previously. A typical example is the IG event recorded in the west Pacific off Japan and the Philippines on 5 January 2008, caused by swells on the North American coast, on the other side of the basin, 10000 km away and one day earlier.

The most energetic FIG events are associated with long period swells reaching a long stretch of shoreline. The model and the few available data support a similar behavior for the North Atlantic, and the model suggests the same for the South Atlantic and Indian oceans, with FIG energy generally radiating from east to west.

Acknowledgments

This work would not have been possible without the bottom pressure data collected by the NGDC together with efforts to maintain the DART network and keeping the observation database. "National Oceanic and Atmospheric Administration (2014): Tsunameter (DART) Data. National Data Buoy Center. Data set accessed at http://www.ndbc.noaa.gov/dart.shtml". We thank the crews and scientific parties that made possible the deployment and recovery of bottom sensors deployed as part of the Graviluck and NEAREST campaigns (project reference, FP6-2005-GLOBAL-4 (OJ 2005 C 177/15, contract 037110) and the German DEPAS instrument pool. F. Ardhuin is funded by ERC grant 240009 for IOWAGA, CNES as part of the SWOT preparation program Labex Mer under grant ANR-10-LABX-19-01 and ANR grant ANR-14-CE01-0012. A. Rawat's grant is co-funded by the CNES and the U.S. National Ocean Partnership Program, under grant N00014-10-1-0383.Comments by two anonymous reviewers led to significant improvements in the manuscript.

Lisa Beal thanks two anonymous reviewers for their assistance in evaluating this manuscript.

References

Alsdorf, D., L.-L. Fu, N. Mognard, A. Cazenave, E. Rodriguez, D. Chelton, and D. Lettenmaier (2007), Measuring global oceans and terrestrial fresh water from space, *Eos*, *88*(24), 253–257.

Ardhuin, F., A. Rawat, and J. Aucan (2014), A numerical model for free infragravity waves: Definition and validation at regional and global scales, *Ocean Model.*, *77*, 20–32.

Ardhuin, F., J. Tournadre, P. Queffelou, and F. Girard-Ardhuin (2011), Observation and parameterization of small icebergs: Drifting breakwaters in the southern ocean, *Ocean Model.*, *39*, 405–410.

Aucan, J., and F. Ardhuin (2013), Infragravity waves in the deep ocean: An upward revision, *Geophys. Res. Lett.*, *40*, 1–5, doi:10.1002/grl.50321.

Ballu, V., et al. (2009), A seafloor experiment to monitor vertical deformation at the Lucky Strike volcano, Mid-Altantic Ridge, *J. Geod.*, doi:10.1007/s00190-008-0248-3.

Biesel, F. (1952), Equations generales au second ordre de la houle irreguliere, *Houille Blanche*, *5*, 372–376.

Bromirski, P. D., O. V. Sergienko, and D. R. MacAyeal (2010), Transoceanic infragravity waves impacting antarctic ice shelves, *Geophys. Res. Lett.*, *37*, L02502, doi:10.1029/2009GL041488.

Cooper, A., D. Jackson, and S. Gore (2013), A groundswell event on the coast of the British Virgin Islands: Variability in morphological impact, *J. Coastal Res.*, *65*, 696–701.

©2014. American Geophysical Union. All Rights Reserved.

Dao, M. H., and P. Tkalich (2007), Tsunami propagation modelling - a sensitivity study, *Nat. Hazards Earth Syst. Sci.*, *7*, 741–754, doi:10.5194/nhess-7-741-2007.

Godin, O. A., N. A. Zabotin, A. F. Sheehan, and J. A. Collins (2014), Interferometry of infragravity waves off new zealand, *J. Geophys. Res. Oceans*, *40*, 1103–1122, doi:10.1002/2013JC009395.

Hanafin, J., et al. (2012), Phenomenal sea states and swell radiation: A comprehensive analysis of the 12-16 February 2011 North Atlantic storms, *Bull. Am. Meteorol. Soc.*, *93*, 1825–1832.

Harmon, N., T. Henstock, M. Srokosz, F. Tilmann, A. Rietbrock, and P. Barton (2012), Infragravity wave source regions determined from ambient noise correlation, *Geophys. Res. Lett.*, *39*, L04604, doi:10.1029/2011GL050414.

Harris, D., L. Matias, L. Thomas, J. Harwood, and W. H. Geissler (2013), Applying distance sampling to n whale calls recorded by single seismic instruments in the northeast Atlantic, *J. Acoust. Soc. Amer.*, *134*(5), 3522–3535.

Herbers, T. H. C., and R. T. Guza (1991), Wind-wave nonlinearity observed at the sea floor. part I: Forced-wave energy, *J. Phys. Oceanogr.*, *21*, 1740–1761. [Available at http://journals.ametsoc.org/doi/pdf/10.1175/15200485%281991%29021%3C1740%3AWWNOAT%3E2.0.CO%3B2.]

Herbers, T. H. C., and R. T. Guza (1992), Wind-wave nonlinearity observed at the sea floor. part II: Wavenumbers and third-order statistics, *J. Phys. Oceanogr.*, *22*, 489–504. [Available at http://ams.allenpress.com/archive/1520-0485/22/5/pdf/i1520-0485-22-5-489.pdf.]

Herbers, T. H. C., S. Elgar, and R. T. Guza (1994), Infragravity-frequency (0.005-0.05 Hz) motions on the shelf, part I, forced waves, *J. Phys. Oceanogr.*, *24*, 917–927. [Available at http://journals.ametsoc.org/doi/pdf/10.1175/15200485%281994%29024%3C0917%3AIFHMOT%3E2.0.CO%3B2.]

Herbers, T. H. C., S. Elgar, and R. T. Guza (1995), Infragravity-frequency (0.005-0.05 Hz) motions on the shelf. part II: Free waves, *J. Phys. Oceanogr.*, *25*, 1063–1079. [Available at http://journals.ametsoc.org/doi/pdf/10.1175/15200485%281995%29025%3C1063%3AIFHMOT%3E2.0.CO%3B2.]

Hoeke, R. K., K. McInnes, J. Kruger, R. McNaught, J. Hunter, and S. G. Smithers (2013), Widepread inundation of Pacific Islands by distant-source wind-waves, *Global Planet. Change*, *108*, 1–11.

Holman, R., and A. J. Bowen (1984), Longshore structure of infragravity wave motions, *J. Geophys. Res.*, *89*, 6446–6452, doi:10.1029/JC089iC04p06446.

Holtman-Shay, J., and R. T. Guza (1987), Infragravity edge wave observations on two California beaches, *J. Phys. Oceanogr.*, *17*, 644–663.

Lefevre, J. M. (2009), High swell warnings in the Caribbean Islands during March 2008, *Nat. Hazards*, *49*, 361–370.

Munk, W. H. (1949), Surf beat, *Eos. Trans. AGU*, *30*, 849–854.

Okihiro, M., R. T. Guza, and R. J. Seymour (1993), Excitation of seiche observed in a small harbor, *J. Geophys. Res.*, *98*(C10), 18,201–18,211, doi:10.1029/93JC01760.

Rascle, N., and F. Ardhuin (2013), A global wave parameter database for geo physical applications. part 2: Model validation with improved source term parameterization, *Ocean Model.*, *70*, 174–188.

Sheremet, A., T. Staples, F. Ardhuin, S. Suanez, and B. Fichaut (2014), Observations of large infragravity-wave run-up at banneg island, france, *Geophys. Res. Lett.*, *41*, 976–982, doi:10.1002/2013GL058880.

Symonds, G., D. A. Huntley, and A. J. Bowen (1982), Two-dimensional surf beat: Long wavegeneration by a time-varying breakpoint, *J. Geophys. Res.*, *87*, 492–498, doi:10.1029/JC087iC01p00492.

Thomson, J., S. Elgar, B. Raubenheimer, T. H. C. Herbers, and R. T. Guza (2006), Tidal modulation of infragravity waves via nonlinear energy losses in the surfzone, *Geophys. Res. Lett.*, *33*, L05061, doi:10.1029/2005GL025514.

Tolman, H. L., et al. (2014), User manual and system documentation of WAVEWATCH-IIITM version 4.18. *Tech. Rep. 316*, NOAA/NWS/NCEP/MMAB.

Tucker, M. (1950), Surf beats: Sea waves of 1 to 5 min. period, *Proc. R. Soc. London, Ser. A*, *202*, 565–573.

Webb, S., X. Zhang, and W. Crawford (1991), Infragravity waves in the deep ocean, *J. Geophys. Res.*, *96*, 2723–2736, doi:10.1029/90JC02212.

©2014. American Geophysical Union. All Rights Reserved.